Laser ablation of a solid target in liquid medium for beryllium nanoparticles synthesis

Sasa-Alexandra Yehia, Lavinia Gabriela Carpen, Flavian Stokker-Cheregi, Corneliu Porosnicu, Veronica Satulu, Cornel Staicu, Bogdan Butoi, Iulia Lungu, Francois Virot, Christian Grisolia, et al.

Nuclear Materials and Energy 31 (2022) 101160

Contents lists available at ScienceDirect

Nuclear Materials and Energy

journal homepage: www.elsevier.com/locate/nme

Laser ablation of a solid target in liquid medium for beryllium nanoparticles synthesis

Sașa-Alexandra Yehia [a,b], Lavinia Gabriela Carpen [a,b,*], Flavian Stokker-Cheregi [a], Corneliu Porosnicu [a], Veronica Sătulu [a], Cornel Staicu [a,b], Bogdan Butoi [a], Iulia Lungu [a], François Virot [c], Christian Grisolia [d], Gheorghe Dinescu [a,b]

[a] National Institute for Laser, Plasma and Radiation Physics, 77125, Magurele, Bucharest, Romania
[b] Faculty of Physics, University of Bucharest, 77125, Magurele, Bucharest, Romania
[c] Institut de Radioprotection et de Sûreté Nucléaire (IRSN) (IRSN, PSN-RES/SAM), 13115 Saint Paul lez Durance, France
[d] CEA, Institut de Recherche sur la Fusion par Confinement Magnétique (IRFM), 13108 Saint Paul lez Durance, France

ARTICLE INFO

Keywords:
Beryllium dust
Laser ablation in liquid
Deuterium retention
Nuclear fusion
Plasma facing materials

ABSTRACT

In this paper, we describe a method to synthesize beryllium (Be) nanoparticles (NPs) by laser ablation of a solid target immersed in a liquid medium. Beryllium dust was successfully synthesized following the irradiation of a Be bulk target, which was immersed in water, acetone or heavy water, respectively, using the first and second harmonic (1064 and 532 nm) of a Nd: YAG laser source providing ns pulses, with a repetition rate of 10 Hz. The laser fluences used for Be target ablation were 8 and 15 J/cm^2. In order to argue the successful obtaining of Be dust, scanning electron microscopy (SEM) was used for surface analysis. Colloidal solutions analysis by dynamic light scattering (DLS) supports the SEM analysis in terms of NPs size, whereas chemical analysis by X-ray photoelectron spectroscopy (XPS) was used in order to investigate the chemical composition. Moreover, thermal desorption spectroscopy (TDS) was performed on Be dust synthesized in heavy water to study the retention of deuterium (D). The key parameters for obtaining much sharper and regular size distribution were identified as being the liquid medium, laser fluence, and wavelength.

Introduction

A problem arising in tokamak-based nuclear fusion reactors is that even if the fusion plasma is magnetically confined, some of the particles escape from the magnetic trap and interact with the walls of the reactor chamber resulting in its erosion. The sputtered material may give rise to deposits and dust. As a consequence, a marked deterioration of plasma facing components (PFCs) is expected, as well as the likely contamination of the fusion plasma itself [1,2] that can lead to major unwanted events as disruption. In the divertor part of the future nuclear fusion reactor (ITER), the plasma facing material (PFM) will be made from tungsten (W) and will be submitted to high heat loads (up to 10–15 MW/m^2). The other part (the blanket), which is submitted to reduced heat loads, is planned to be constructed with 440 panels, which will be coated with an 8–10 mm layer of Be [3]. The decision to use Be on most of the surface exposed to the fusion plasma was made, taking into account its low degree of erosion by chemical and physical interaction, small mass number, which improves the reactor tolerance to higher concentrations of Be impurities in plasma, as opposed to high-Z counterparts such as W [4], high thermal conductivity, and low retention rate of hydrogen isotopes compared to the other materials used in tokamak [5].

One of the main disadvantages of Be is that in the form of particles, in the case of inhalation, is toxic [6]. Another disadvantage is the low melting temperature (1560 K), compared to other potential materials to be used in the reactor chamber, such as W. While W and C have been extensively studied, the knowledge on Be dust creation processes in a plasma environment is more limited [7].

Beryllium particles can be expelled from the First Plasma Wall (FPW) during plasma operation due to ELMs (Edge-Localized Modes) [8] and imperfect plasma confinement. These Be particles can pose serious problems as a result of their redeposition in remote areas, changing the inner wall properties, but also due to their negative impact on diagnostic equipment. The hydrogen isotopes, deuterium and tritium, used as fuels for a fusion reactor, can be implanted into Be first wall [9] due to their

* Corresponding author at: National Institute for Laser, Plasma and Radiation Physics, 77125, Magurele, Bucharest, Romania.
E-mail address: lavinia.carpen@inflpr.ro (L.G. Carpen).

https://doi.org/10.1016/j.nme.2022.101160
Received 19 January 2022; Received in revised form 2 March 2022; Accepted 3 March 2022
Available online 5 March 2022

escaping from the main fusion plasma. Some studies [9,10] explored the effect of Be impurities in deuterium plasma as a consequence of erosion after plasma-materials interaction. Thus, the study of the interaction between Be and hydrogen isotopes, and the removal of the retained isotopes are a priority for the proper functioning of future fusion reactors.

The main information about Be used in fusion technology were provided by the Joint European Torus (JET) experimental reactor. It was found that using Be as material for the first wall, both in the form of bulk as well as in the form of thin layers, led to an improvement of plasma parameters [11] manifested by increasing the density of deuterium ions, the ion temperature, and the confinement time.

In this study, we used the pulsed laser ablation (PLA) method in a liquid medium to synthesize Be NPs from a solid Be target immersed in different liquids. Beside multiple similarities between the pulsed laser ablation in gas and liquid, an important difference is that the liquid strongly confines the plasma plume onto the ablation area. This confinement slows down the cooling rate at the interface between the ablated material and the target. The hot ablated material can provide thermal energy to the underlying target and a larger portion of the target reaches the energy threshold for detachment [12]. Thus, the ablation yield in liquid is higher than in gas. This method is based on a simple experimental setup through we have the possibility to obtain NPs from a wide range of materials (metals, polymers etc.). We chose the liquid phase because Be dust is deemed toxic for the human body and the environment, whereas the confinement of oxide NPs to a colloidal environment eliminates the risk of inhalation of toxic substances. As compared to dry NPs, colloids are easier and safer to handle [13].

Based on high toxicity and environmental problems raised, the scientific literature on Be and Be oxides (BeO) particles synthesis is limited. The traditional methods for BeO NPs synthesis used chemical processes which include sol–gel route [14–16]. Using this method, BeO was synthesized in the form of nano powder with small particle diameters, under 50 nm, partially agglomerated. Additional step which includes calcinations is required in order to accomplished a uniform morphology and size distribution [16]. These studies point out the ease of execution and the versatility of the laser ablation process in liquid in relation with traditional methods used for Be NPs synthesis. This aspect represents another reason for our choice to use PLA method in a liquid environment for Be particles synthesis.

The processes that govern NPs formation using PLA method in a liquid medium can be summarized as follows [17–19]: 1) the laser beam is focused on the target surface, which is immersed into the liquid, producing the photoionization; 2) after the ionization process, some material from the surface target will detach by plasma formation, thermal or a thermal mechanism, shock waves, etc. The energy released by the plasma plume in the liquid leads to the formation of bubbles; 3) NPs are generated due to the ejected material from the target surface captured by the bubbles and released into the liquid after the bubbles break.

Metal NPs have already been synthesized by laser ablation in various liquids (water, ethanol, isopropyl alcohol etc.) [20], but there are few studies on the obtaining of Be NPs by this method. Barmina et al. [21] showed in their work the successful obtaining of Be NPs by PLA, for application regarding gamma activity decreasing. Sukhov et al. [22] studied the hydrogen generation by laser irradiation of iron and beryllium colloids in water. They synthesized beryllium and iron particles by ablation of solid targets in liquid using an ytterbium-doped laser (1060–1070 nm), with 8 ns laser pulse duration and 200 kHz pulse repetition rate. The pulse energy was 0.1 mJ and the exposure time was about 2 min. The Be NPs have average sizes of about 35 nm, but they also found particles with sizes of about 450 nm. For the same condition, iron NPs have average sizes of about 20 nm to 50 nm. Stokker-Cheregi et al. [23] studied the feasibility of the laser ablation of metallic W and Al targets immersed in acetone and water, as a technique for producing NPs using the second harmonic of a Nd: YAG laser at 532 nm, with a pulse of 7 ns, and a frequency of 10 Hz, at exposure time of 30 min (18.000 pulses). The average of W and Al NPs sizes obtained by this method varied between 50 and 70 nm.

The scope of our work relates to the broader study of chemical and physical properties of Be dust, particularly in view of their future practical implications in the functioning of tokamak nuclear fusion reactors, as material used in the inner wall. Our approach of using PLA in liquid medium in order to synthesize NPs has several advantages: i) it is safe and easier to handle compared to dry NPs [13]; ii) it has low/moderate cost; iii) it is easy to implement in order to expand current research in this relatively unknown area; iv) a higher ablation yield than in gas due to the fact that a larger surface of the target reaches the energy threshold for detaching [12]. These criteria are interlocked when considering a particular approach and design decision, and this will always involve trade-offs between the considered aspects in order to achieve a feasible solution for the production of Be dust by laser ablation in liquids. Moreover, the study of D retention in Be dust synthesized by PLA in heavy water was also investigated by TDS analysis. Compared to other experimental methods which incorporate D by bombarding the bulk Be target with monoenergetic ion beams in UHV conditions [24,25], our approach is a new method which allows both the synthesis of Be NPs and the incorporation of D into Be dust in a single step.

Material and methods

General principles and design of the experimental setup

Beryllium particles were synthesized by laser ablation of a Be bulk target in different aqueous media, such as acetone, bi-distilled water, and heavy water. The experimental setup used for this application is presented in Fig. 1 and includes a Q-switched high-power Nd: YAG laser (Quantel) used as energy source providing ns laser pulses, operating at 10 Hz pulse repetition rate, which was tuned to work at wavelengths of 1064 and 532 nm. A dichroic mirror used to deflect the laser beam vertically is mounted on a computer-controlled stage providing X-Y scanning of the laser beam across the surface of the target. The laser beam was focused using an objective (fused silica lens with focal distance f = 30 cm) onto the surface of the target. The Be target having 2-inch diameter and 99.0 % purity is placed at the bottom of a tall vessel, which has a height of 15 cm and a diameter of 7 cm, on a Teflon holder immersed in liquid. The vessel is mounted on a rotating stage ensuring a homogeneous ablation of the target across an area about 2 cm in diameter. That being said, there will be a compromise due to the fact that Be erosion in fusion tokamak reactors is expected to evolve in non-equilibrium plasma and the fact that the experimental system must be safe for our approach.

In general, the energy of the laser pulses can be attenuated by directly adjusting the laser operating parameters of the laser source (flash-lamp voltage, Q-switch delay, etc.), or by passive optical components, such as filters. An important priority for the safe operation of high-power lasers is the removal of reflections produced by additional optical components. These reflections are extremely damaging for the optical components and for the laser source, and not at least for the operators of the experimental setup. Therefore, in our experimental approach, the attenuation of the laser beam intensity was based on the adjustments of the Q-switch delay, which eliminated the need for filters and their associated risks. Another important priority is to avoid the contamination of users with the Be dust due to the fact that the vessel in which the solid target was placed is open. For this top priority, we have performed preliminary experiments using an aluminum target to observe at which wavelengths, fluences, and liquid parameters the ablation procedure can be carried out without any contamination from ejected droplets of colloids. The correspondences between laser Q-switch delay and pulse energy for 1064 nm and 532 nm operating wavelengths used to ablate Be bulk target in liquid are presented in Table 1.

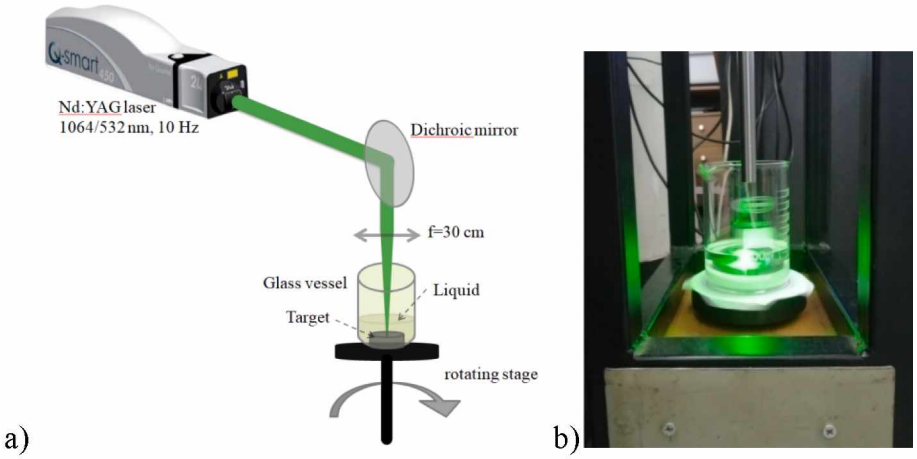

Fig. 1. a) Experimental setup and b) image of the Be bulk target ablated in liquid medium.

Table 1
Laser pulse parameters used for Be target ablation in liquid.

Laser wavelength (nm)	Q-switch delay (μs)	Pulse energy (mJ)
532	200	47
	175	83
1064	210	41
	185	79

It should be noted that high-power lasers have pulse-to-pulse energy fluctuations of around 5 % when operating in optimal conditions. These fluctuations can increase to around 10 % when the Q-switch delay is adjusted for tuning the pulse energy.

The laser fluence for a pulse energy of 45 mJ is around 8 J/cm^2, whereas for a pulse energy of 80 mJ is around 15 J/cm^2. For the laser fluence of 8 J/cm^2, the target needs to be immersed in 80 mL of liquid, and for a laser fluence of 15 J/cm^2 in 100 mL of liquid, in order to prevent the ejection from the glass vessel of the toxic droplets, thus ensuring a safe operation of the experiment. These parameters were established, in order to avoid any contamination of the uses, during a preliminary experiment, performed on an Al target.

We have chosen the ablation time based on preliminary tests performed with Al targets in conditions similar to those used for Be. Thus, we performed the ablation experiments in acetone and bi-distilled water and we identified that after 10 min, the NPs are difficult to be observed, while after 30 min, the NPs were already synthesized. Accordingly, we established a reasonable ablation time of 20 min in acetone and bi-distilled water. Moreover, with respect to the experiments which involve in one step both synthesis of Be NPs and deuterium incorporation, we established a longer ablation time of 80 min, to be sure that we collect enough deuterated material for analyses.

The experimental conditions for the Be NPs synthesized by PLA are presented in Table 2.

Liquid medium

The liquid media used for laser ablation of Be bulk target were bi-distilled water, acetone (C_3H_6O), and heavy water (D_2O), selected due to the fact that these liquids can form stable nanoparticles colloids for a long time with small agglomerates in solution [26]. The solvents can influence the particle size distributions and the stabilization by anion adsorption (in acetone), surface oxidation or by hydroxide shells formed (in water) [26].

Material characterization

The surface of the NPs was analyzed by an FEI Inspect S Scanning Electron Microscope using thermal emission filament. The electron acceleration voltage varied between 0 and 15 kV on a working distance in the range of 0 – 30 mm under high vacuum conditions.

The dynamic light scattering studies were carried out for size distribution analysis using Horiba Scientific SZ-100, Malvern Instruments equipment. Measurements were performed on colloidal samples resulting from laser ablation experiments performed only in bi-distilled water. Three measurements were acquired for each sample and all measurements were done at 25 °C. We did not performe DLS measurements in acetone because the available containers, in which the colloidal solution was stored, chemically react with this liquid medium.

The chemical composition was determined by XPS analysis using a K-Alpha Thermo Scientific (ESCALAB™ XI) spectrometer. XPS spectra were acquired using a monochromatic Al Kα X-ray source (1486.68 eV) and a X-ray spot of 900 μm diameter. An electron flood gun has been used for charging effect compensation of the Be NPs surface. For the correction of charging effects during acquisition, all spectra were calibrated using the C 1 s peak at 284.8 eV. A pass energy of 50 eV was employed for the survey spectrum, while 20 eV and 50 scans were used for the C1s, O1s, and Be1s narrow spectra. An energy step size of 0.1 and

Table 2
Experimental conditions of the Be NPs synthesized by PLA.

Liquid type	Laser wavelength (nm)	Pulse energy (mJ)	Fluence (J/cm^2)	Volume (mL)	Treatment time (min)
Be dust production					
Acetone (C_3H_6O)	532	47	8	80	20
		83	15	100	
Bi-distilled water	532	47	8	80	
		83	15	100	
	1064	41	8	80	
		79	15	100	
Retention of deuterium in Be dust					
Heavy water (D_2O)	1064	79	15	100	80

1.0 eV for high resolution and survey spectra were used, respectively. Both recording and processing, low and high resolution XPS spectra, were performed using advanced Avantage software (Thermo Avantage v 5.976, Thermo Fisher Scientific, East Grinstead, UK).

Investigation of D retention and inventory was performed through TDS measurements. The Be dust was loaded in a quartz tube connected to a quadrupole mass spectrometer (QMS) and a turbo molecular vacuum system, in order to achieve a working base pressure of 10^{-6} Pa. Afterwards, samples were individually transported to the measurement area of the quartz tube and heated by means of a temperature-controlled oven, adjusted to maintain a stable 10 K/min until reaching the final programmed temperature of 1050 °C.

Results and discussion

SEM analysis reveals that Be NPs were not obtained when acetone is the liquid medium for laser ablation method. We noticed a modification of the Be surface in the region irradiated by the laser pulses (Fig. 2a-e), which indicates the formation of a carbon layer on the top of the target (Fig. 2b), whereas neither NPs nor colloidal solution were observed in liquid by DLS. The presence of the carbon layer is explained by the dissociation process of the acetone molecules in the generated plasma plume and redeposition of the fragments on the target surface [23,27]. The results were similar for both considered laser fluences used in the experiments (8 and 15 J/cm^2). These results were also supported by the target mass, which increases after 20 min of laser ablation. In accordance with the target mass and the problems encountered during DLS measurements, we consider that acetone is not suitable for this study, and further experiments have focused on bi-distilled water and heavy water.

In the case of using bi-distilled water as a liquid medium, after 20 min (~12000 laser pulses) of Be target ablation, we noticed the formation of a clearly discernible colloidal solution (Fig. 2e). The estimation of the ablation rate was performed by weighing the Be target after each experiment. For laser ablation in bi-distilled water for 20 min at laser fluence of 15 J/cm^2, 1 mg of lost material is obtained. In other words, the ablation rate is approximately 8.33×10^{-5} mg/pulse in bi-distilled water.

Laser parameters modified NPs sizes

To identify the size of the NPs, a small amount of colloid was taken and cast on silicon substrates. Before SEM analysis the liquid must be evaporated. The analysis shows that in the case of laser ablation of a target in bi-distilled water, carried out using laser wavelengths of 532 and 1064 nm as well as laser fluences of 8 and 15 J/cm^2, the majority of the Be NPs have sizes between 50 and 100 nm (Fig. 3).

The NPs size distribution and the average size were estimated by ImageJ (image processing program [28]). Fig. 4 illustrates the frequency of particles number as a function of particles size in order to determine the average size and the distribution functions. The shapes of the distribution curves indicate that the number of particles of the order of tens of nanometers is limited, and not only nanoparticles are formed, but larger particles as well.

In terms of particles size, in addition to the SEM analysis, DLS measurements were performed. It is observed that Be NPs, synthesized by laser ablation in a liquid medium, show a tendency to agglomerate. This behavior is characterized by the hydrodynamic diameter, which reaches a minimum value of 1958.3 ± 524 nm, in the case of the sample obtained after laser ablation at 1064 nm with a fluence of 15 J/cm^2. The other samples, obtained at low laser wavelength and low fluence, respectively, present a much higher hydrodynamic diameter (Fig. 5, black line).

The polydispersity index (PDI) (Fig. 5, red line), which is the measure of the heterogeneity (diversity) of NPs based on size, follows the same tendency as the hydrodynamic diameter and thus, we can claim that the samples resulting from the laser interaction with Be target, when a low wavelength and low fluences are used, are characterized by an extremely polydisperse suspension. The polydispersity index that reaches values even higher than three is translated into the fact that there are multiple populations in the sample with different particle sizes and these samples are not suitable for DLS characterization. This index reaches the minimum value of 0.847 ± 0.1054 in the case of the sample obtained at high wavelength and high energy/pulse. Even if this value indicates that the sample is still characterized by a broad size distribution, the sample is suitable for DLS characterization.

By comparing DLS and SEM data, the aggregation state of NPs can be easily determined. It was observed that the diameter of particles measured by DLS is larger than SEM size analysis. Therefore, the colloidal solutions obtained after laser interaction with Be target, in bi-distilled water are in aggregated form.

Summarizing the obtained results, we noticed that the process of NPs synthesis in liquid by laser ablation is influenced by the properties of the liquid medium and the laser parameters. First, we evidenced that that acetone is not useful for this type of process. We observed also that the higher laser fluence leads to larger nanoparticles. The laser fluence affects the thermodynamics of the plasma formed after laser-target interaction and the dynamics of the cavitation bubbles. When the laser fluence is high, the plasma plume has a higher pressure and temperature, and the bubbles are lasting for a longer time before collapsing [27].

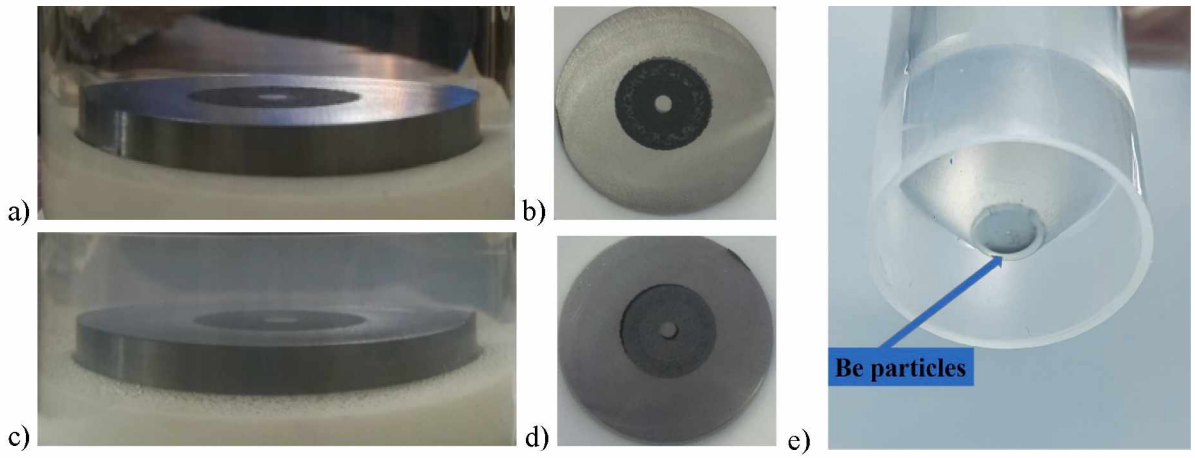

Fig. 2. Images of Be target ablated in acetone (a, b) and in bi-distilled water (c, d), and e) image of a deposit obtained after the sedimentation of Be particles obtained in bi-distilled water.

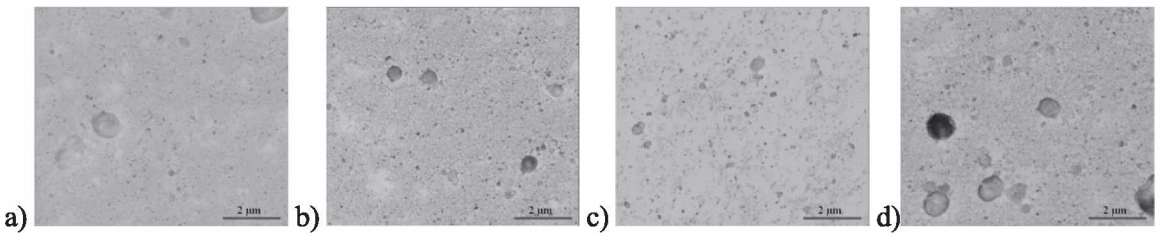

Fig. 3. SEM images of Be NPs synthesized by laser ablation in bi-distilled water at wavelengths and laser fluences of a) 532 nm and 8 J/cm^2, b) 532 nm and 15 J/cm^2, c) 1064 nm and 8 J/cm^2, d) 1064 nm and 15 J/cm^2.

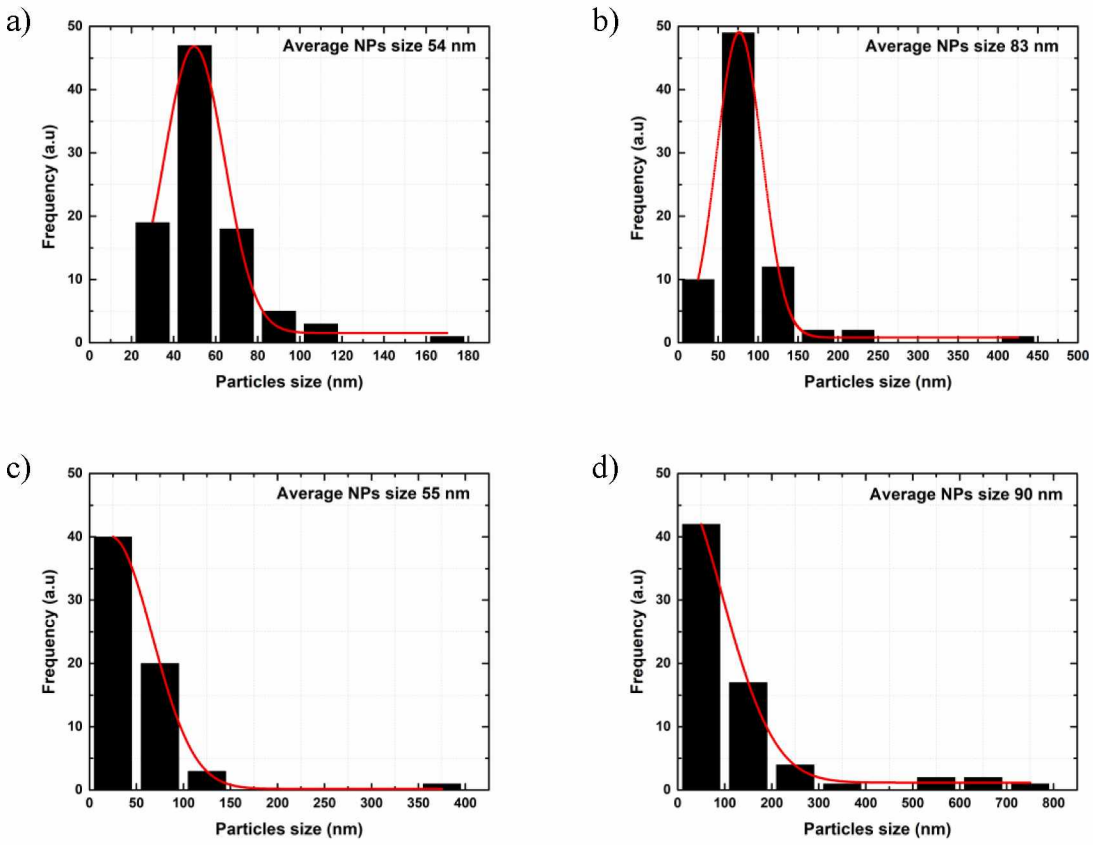

Fig. 4. Size distributions of Be NPs synthesized in bi-distilled water at wavelengths and laser fluences of a) 532 nm and 8 J/cm^2, b) 532 nm and 15 J/cm^2, c) 1064 nm and 8 J/cm^2, d) 1064 nm and 15 J/cm^2.

These conditions favor the particle's coalescence. Another factor that can affect the size of the Be NPs, by decreasing it, is the laser-induced fragmentation [27]. of the already formed particles by absorption of the laser energy of the next pulses. However, the results indicate that in the present conditions the fragmentation is enough important to counterbalance the effect of fluence. Laser wavelengths can also influence the particles size [29], due to Bremsstrahlung absorption [30] or optical absorption [31]. In our case, the differences between the NPs size formed at 532 nm and at 1064 nm are very small and can be neglected. Taking into account all these observations, both laser wavelengths and laser fluences are suitable for particles production by laser ablation in bi-distilled water.

Nevertheless, at higher fluence and wavelength, the agglomeration tendency is not so accentuated, as indicated by the DLS measurements. Given the purpose of the experiment and taking into account the results obtained using SEM and DLS techniques, we went further by selecting just a series of experimental parameters (1064 nm, 15 J/cm^2). We continued the experiment using heavy water as liquid medium in order to incorporate deuterium atoms in synthesized nanoparticles.

Bi-distilled water versus heavy water as liquid medium

The experiment with heavy water (48000 pulses were used) achieved much uniform size distribution (Fig. 6). The average of NPs size is around 80 nm, but the distribution curve is much larger than the distribution curves of NPs synthesized in bi-distilled water. This result indicates that the laser ablation of Be target in heavy water generates a lot of particles with sizes below 100 nm, with the majority of particles of the order of tens of nanometers.

X-ray Photoelectron Spectroscopy technique was used to determine the surface elemental composition and to establish the elemental bonding states at the surface of the obtained Be NPs. The spectra will be presented below, by comparison, between samples synthesized in bi-distilled and in heavy water media. Survey spectra, presented in

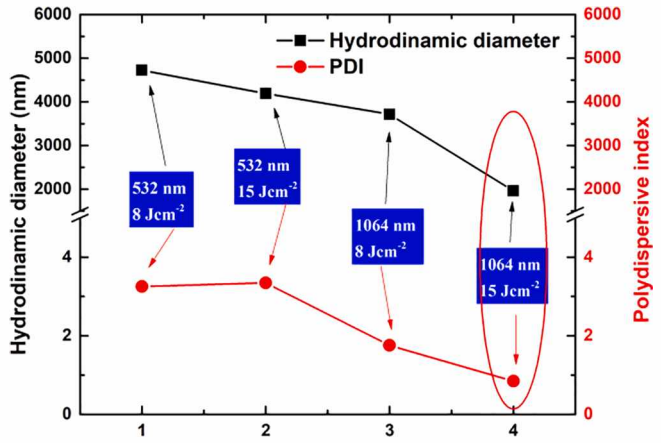

Fig. 5. DLS measurements of Be NPs synthesized by laser ablation in bi-distilled water.

Fig. 7, revealed on the Be NPs surface, the presence of Be1s and O1s as the most prominent lines for both samples synthesized in bi-distilled water and heavy water at 1064 nm with fluence of 15 J/cm^2. C1s line is also present at the Be NPs surface as an impurity originating from the adventitious carbon.

The surface relative atomic composition of the samples synthesized in bi-distilled water and in heavy water determined from the interpretation of XPS survey spectra, is reported in Table 3.

The high-resolution spectra for Be1s, recorded for the Be NPs synthesized in bi-distilled water and in heavy water, which reveal some variations with respect to the used liquid medium, are displayed in Fig. 8a. Typical deconvolutions of the Be1s high resolution spectra of the sample synthesized in bi-distilled water and heavy water are depicted in Fig. 8b and Fig. 8c. The spectra were normalized for a better comparison of the modifications induced by the liquid media.

The Be1s spectrum recorded for the Be NPs synthesized in bi-distilled water present a shoulder towards higher binding energy, which suggests some surface contamination. The deconvolution of Be1s spectrum recorded for Be NPs dispersed in bi-distilled water was fitted using three singlets, and are assigned as follows: an important contribution of 53.37 % is devoted to metallic Be (111.54 eV), a contribution of 27.94 % is assigned to BeO bonds, and a contribution of 18.7 % which is related to surface contamination bonds.

The deconvoluted spectrum of Be1s recorded for the Be NPs synthesized in heavy water reveals a mixture of metallic Be, with the most important contribution of 79.07 %, BeO with a contribution of 20.59 %, and Be contamination bonds with a very insignificant contribution (0.34 %). From the chemical bonding states of the synthesized Be NPs, it is easily observed that a higher contribution of Be in the metallic state is attained for the sample synthesized in heavy water. Thus, we can conclude that heavy water plays an important role on the formation of Be NPs with higher content of metallic Be and with stable surface regarding the contamination. Even if the chemical composition of Be NPs obtained by our method is far from the one obtained in tokamak, the

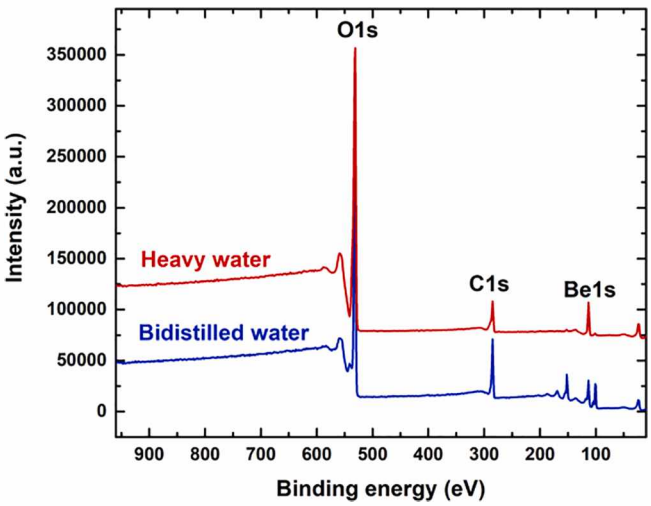

Fig. 7. Survey spectra for samples synthesized in bi-distilled water and heavy water.

Table 3
Atomic concentration of the elements present on the Be NPs surface.

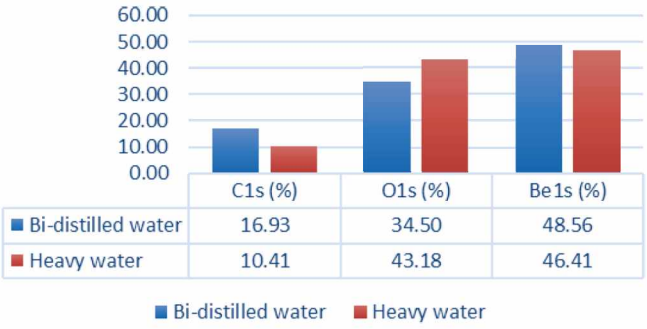

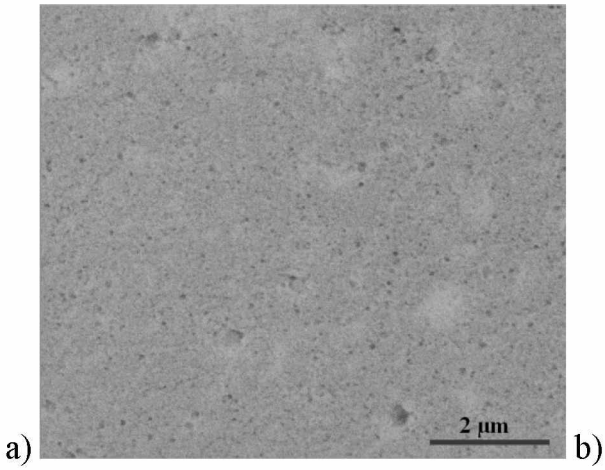

Fig. 6. a) SEM images, and b) size distributions of Be NPs synthesized by laser ablation in heavy water.

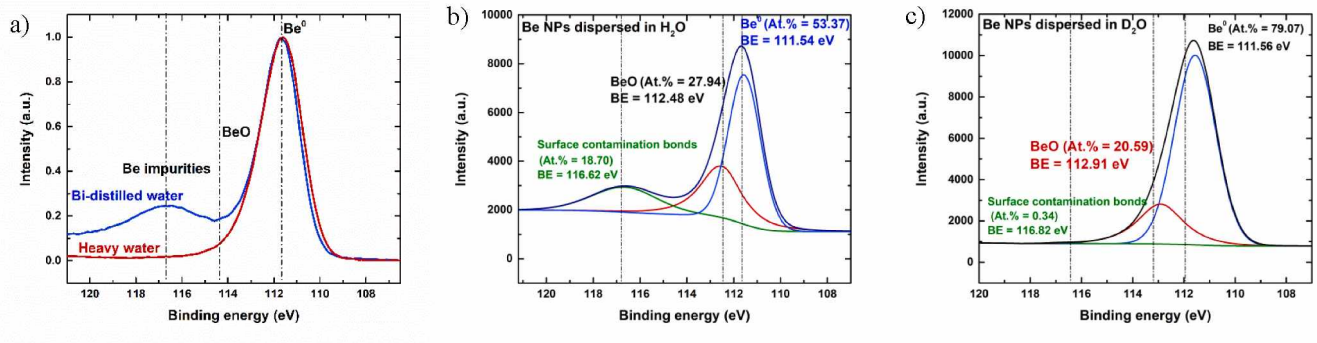

Fig. 8. a) High-resolution spectra for Be NPs synthesized in bi-distilled water and heavy water and b) the deconvolutions for Be1s energy region recorded for bi-distilled water and c) heavy water.

chemical composition of these NPs is relevant. The Be NPs formed in heavy water contain almost 80 % metallic Be (after high-resolution XPS spectra deconvolution), which is a promising result for NPs obtained in liquid medium.

Deuterium retention in Be dust NPs

The basic mechanism for Be NPs synthesized by PLA involved laser target interaction, plasma generation, the formation of bubbles, and the releasing of NPs in solution [32]. Regarding D retention in Be NPs, we assume that during the formation of the bubble cavity in heavy water, D atoms formed by dissociation processes can be tied to Be atoms expelled from the target and captured in bubbles. These being said, the Be NPs released in the liquid are deuterated. An important observation is that most of the NPs synthesized in liquid media have an excess of electrons that prevent the aggregation during the bubble cavity evolution [33]. However, the mechanism of NPs released from the bubble cavity into solution is not well known, being several theories [34]. Some works suggest that the NPs are released during the collapse stage [35] or they are formed during the expansion inside the bubble cavity [36].

In order to observe the D release behavior and to quantify the D inventory in the samples, TDS measurements were performed.

Before samples measurements, HD and D_2 calibrations were performed in order to accurately quantify the D inventory. These were conducted using two separate gases, molecular hydrogen and deuterium, leaking into the TDS chamber. Their characteristic ion currents are measured using a Pfeiffer Vacuum Quadera QMG 220 QMS provided with a tungsten filament. The parameters of the quadrupole mass spectrometer were the same for both measurements and calibrations performed. The leak into the TDS chamber was controlled using a Mass Flow Controller with step size of 0.01 sccm. This gas leak system ensures good versatility for testing the detection sensibility of the QMS by providing a high number of measurement points over a large interval of partial pressures. In comparison, to leak standards in this configuration a calibration curve was obtained that can support accurate extrapolation of the calibration factor.

The desorption chart in Fig. 9 corresponds to the sample synthesized in heavy water. As we can observe, D is released as HD and D_2 molecules. Hydrogen is present bonded within the released D since, D is desorbed from the sample mainly in atomic state. It quickly recombines in order to reach a steady molecule. The recombination having the highest probabilities are the ones with H isotopes. Thus, the free D atoms will most likely combine with the first H isotopes that they encounter. H is present in the TDS device due to many causes. First of all, it is an intrinsic element for all materials. Secondly, since it is present everywhere, it starts to outgas from all of the TDS device elements during temperature rise. Regarding relatively low D content in the samples, we claim that it was released mostly in the form of HD molecules. This is a common behavior during TDS measurements for low content of D samples. If we

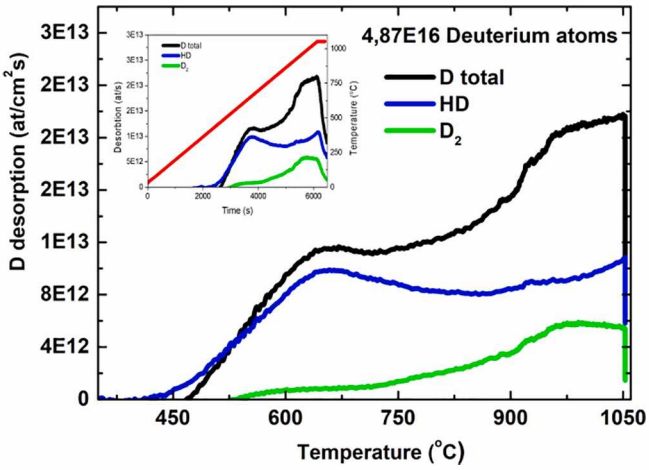

Fig. 9. Deuterium desorption curves (HD, D_2 molecules, and calculated D atoms) for the Be NPs synthesized in heavy water.

carefully analyze Fig. 9, the low temperature peak (625 °C) due to low D content, is released mostly as HD. Rising the temperature, we observe an increase of the D amount due to the recombination mechanism described above, the D_2/HD ratio increases. However, the H amount is not to be taken into account when considering the retention/release mechanisms.

The D atoms curve is calculated and showed in Fig. 9, taking into account the HD and D_2 calibration method mentioned above by adding the number of HD molecules twice as the D_2 molecules corresponding to each temperature. Their behavior is characterized by release onset at 470 °C, one evident broad D peak at 650 °C, followed by an increase of D desorption that is not completed up to the maximum temperature that was achieved, 1050 °C. This behavior suggests that the D is released in two main sequences attributed to separate trapping retention (different D release peaks) mechanisms. Unfortunately, there is no literature data available on D release behavior in Be dust, but if we extrapolate the well-known results for bulk Be [24,25] and Be coated layers [37] we can argue that D is trapped in crystallographic (like vacancy) defects and the network voids of the Be dust. Also, the total amount of D was calculated at 4.87×10^{16} D atoms and represents 0.0025 D:Be ratio. This value is a promising result and this experiment represents a first attempt in obtaining deuterated Be dust by laser ablation in heavy water. Also, the fact that the D desorption is not complete until the maximum temperature, as seen in the inset of Fig. 9, and also during the 10 min hold, demonstrates that the D amount is higher than calculated. D desorption decrease after 1000 °C suggests that, although it is still released, its provenience is from lower temperatures peaks. In addition, the diffusion coefficient of D in Be plays a substantial role in the release curves.

Fig. 10 presents the water and heavy-water desorption signals for the sample synthesized in heavy water obtained by means of TDS. The HDO signal (mass 19) has two relatively sharp peaks at low temperatures (~170 and 290 °C). This fact, corroborated with the D release behavior (absence of 330 °C release peak [24]) suggests that although the laser irradiation was performed under heavy water, no D bonds as Be deuteroxide were determined.

We made a comparison of deuterium retention properties between the existing studies on bulk and layers materials relevant to fusion nuclear field and Be NPs obtained in the present work. Haasz et al. [38] studied the retention of D in Be bulk materials and identified a sharp release at ~ 200 °C followed by two small releases around 400 and 500 °C. The total amount of D retained was 2.7×10^{21} D/m^2 and the D:Be ratio was 0.39. The authors also studied the retention of D in Mo and W bulk materials and identified desorption peaks at around 30 and 400 °C for Mo, respectively around 300 and 500 °C for W. The total amount of D retained in W was 6×10^{20} D/m^2 with D:W ratio of 0.24, and up to 10^{20} D/m^2 for Mo. Manhard et al. [39] indicated D release peaks at 250 and 400 °C for W bulk material. By applying a thermal treatment, the recrystallized W samples present different deuterium release spectra. Deuterium inventory was reduced with the increase of treatment temperature. The total amount of D retained in non-recrystallized samples was about 20×10^{19} D/m^2 and in recrystallized samples, 10×10^{19} D/m^2. De Temmerman et al. [40] studied the retention of D in co-deposited Be layers and identified a D:Be ratio of 0.7 with D release between 30 and 300 °C. Zaloznik et al. [41] observed a sharp desorption peak at 230–260 °C for D incorporated in Be co-deposits at room temperature. For Be co-deposits at higher temperature, D is released at higher temperature (400–500 °C). Reinelt et al. [24] studied the implantation of D in Be bulk material and identified two desorption regions, at ~ 100–200 °C and around 400–500 °C. Moreover, D desorption is complete above 680 °C and the maximum local D:Be ratio is 0.35.

These studies and the fact that, in the present work, D starting to release at 470 °C, followed by an evident broad at 650 °C, and still release up to the maximum device temperature, indicates that our samples liberate D at relatively similar temperatures to bulk or layer materials. In terms of the D:Be ratio, our samples incorporate a small amount of D compared to the cases discussed above, but considering that the desorption is not complete until the maximum temperature, the ratio can be higher than 0.0025. An important aspect is related to the fact that carbon or oxygen impurities which can affect the retention of hydrogen isotopes [42], are only in small amount in our samples. Nevertheless, should be outlined, that the mechanisms of deuterium incorporation in the above-described situations are very different compared with pulsed laser ablation in liquid, being based on temperature [42], ion energy [43], and background pressure [44].

Conclusions

In this study, we have explored the approach of obtaining Be NPs by laser ablation in different types of liquid media. The importance of our results stems from a two-fold interest in this type of material in view of its future applications and implications: on one hand, Be dust is expected to be produced in large quantities in next-generation tokamak-based nuclear fusion reactors, such as ITER. As such, exploring alternative ex-situ approaches towards the production of Be NPs opens up new possibilities to study their properties and functionalities. On the other hand, and equally important, Be dust has been classified as toxic, so our approach of obtaining Be NPs in a controlled environment in which the risk of contamination is eliminated represents a golden opportunity to further expand our knowledge of this dust through subsequent biocompatibility experiments. In addition, the laser parameters (wavelength, pulse duration, fluence, spot diameter, incident angle etc.), the target composition and geometry, and the liquid type can be controlled in order to favorably adjust NPs formation. Our current research allowed

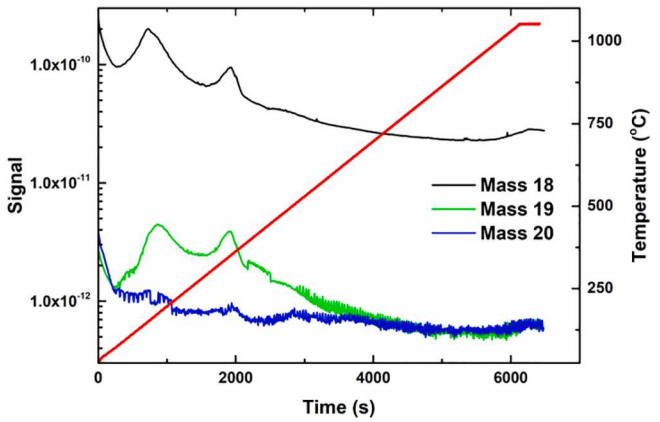

Fig. 10. TDS water desorption signals (H_2O, HDO, and D_2O) for the Be synthesized in heavy water in logarithmic scale.

to synthesize Be NPs with sizes between several tens and hundreds of nm using a versatile and easy-to-use experimental approach that conformed to all safety standards, and we also managed to extract an ablation rate of approximately 8×10^{-5} mg/pulse at a fluence of 15 J/cm^2, for both considered laser wavelengths (532 and 1064 nm, respectively). The chemical analysis of these NPs reveals that Be is indeed their main constituent (over 50 %). The sample obtained in heavy water is distinguished by a high percentage of metallic Be (~80 %), a small contribution of oxygen, and carbon. Therefore, heavy water is the most promising liquid medium for the synthesis of Be NPs by laser ablation. Moreover, heavy water offers the opportunity to incorporate D in material. Thermal desorption measurements were performed on Be dust synthesized in heavy water to study the retention of deuterium. The total amount of D atoms was higher than 4.87×10^{16} and the D:Be ratio, up to 2.5:1000. This value is a promising result and this experiment represents a first attempt in obtaining D loaded Be dust by laser ablation using heavy water.

CRediT authorship contribution statement

Saşa-Alexandra Yehia: Investigation, Data curation, Writing – original draft. **Lavinia Gabriela Carpen:** Investigation, Data curation, Writing – review & editing. **Flavian Stokker-Cheregi:** Conceptualization, Investigation, Writing – review & editing. **Corneliu Porosnicu:** Resources, Writing – review & editing. **Veronica Sătulu:** Investigation, Writing – review & editing. **Cornel Staicu:** Investigation. **Bogdan Butoi:** Investigation. **Iulia Lungu:** Investigation. **François Virot:** Validation, Funding acquisition, Writing – review & editing. **Christian Grisolia:** Validation, Funding acquisition, Writing – review & editing. **Gheorghe Dinescu:** Conceptualization, Supervision, Writing – review & editing.

Declaration of Competing Interest

The authors declare that they have no known competing financial interests or personal relationships that could have appeared to influence the work reported in this paper.

Acknowledgements

This work was supported by Romanian Ministry of Research, Innovation and Digitization, CCCDI—UEFISCDI, in the frame of Nucleus Programme INFLPR LAPLAS VI [grants numbers 16N, 2021]; by French Institute for Radiological Protection and Nuclear Safety (IRSN); and by EUROfusion Consortium and has received funding from the Euratom research and training programme 2014–2018 and 2019–2020 (work package WPEDU-RO, ctr. 1EU-12) under grant agreement No 633053.

The views and opinions expressed herein do not necessarily reflect those of the European Commission.

References

[1] G. Federici, C.H. Skinner, J.N. Brooks, J.P. Coad, C. Grisolia, A.A. Haasz, A. Hassanein, V. Philipps, C.S. Pitcher, J. Roth, W.R. Wampler, D.G. Whyte, Plasma-material interactions in current tokamaks and their implications for next step fusion reactors, Nucl. Fus. 41 (12) (2001), https://doi.org/10.1088/0029-5515/41/12/218.

[2] H. Verbeek, J. Stober, D.P. Coster, W. Eckstein, R. Schneider, Interaction of charge exchange neutrals with the main chamber walls of plasma machines, Nucl. Fusion 38 (12) (1998) 1789–1803, https://doi.org/10.1088/0029-5515/38/12/305.

[3] International Thermonuclear Fusion Experimental Reactor Project 2009 ITER Report, ITER D 2X6K67 v1.0 Plant Description (PD) Cadarache.

[4] J. Linke, J. Du, T. Loewenhoff, G. Pintsuk, B. Spilker, I. Steudel, M. Wirtz, Challenges for plasma-facing components in nuclear fusion, Matter Radiat. Extremes 4 (5) (2019) 056201, https://doi.org/10.1063/1.5090100.

[5] G. De Temmerman, K. Heinola, D. Borodin, S. Brezinsek, R.P. Doerner, M. Rubel, E. Fortuna-Zaleśna, C. Linsmeier, D. Nishijima, K. Nordlund, M. Probst, J. Romazanov, E. Safi, T. Schwarz-Selinger, A. Widdowson, B.J. Braams, H. K. Chung, C. Hill, Data on erosion and hydrogen fuel retention in Beryllium plasma-facing materials Vol. 27 (2021), https://doi.org/10.1016/j.nme.2021.100994.

[6] P.H. Rebut, R.J. Bickerton, B.E. Keen, The Joint European Torus: installation, first results and prospects, Nucl. Fusion 25 (9) (1985) 1011–1022, https://doi.org/10.1088/0029-5515/25/9/003.

[7] E. Bertolini, Impact of JET experimental results and engineering development on the definition of the ITER design concept, Fusion Eng. Des. 27 (1995) 27–38, https://doi.org/10.1016/0920-3796(95)90115-9.

[8] R. Lunsford, A. Bortolon, R. Maingi, D.K. Mansfield, A. Nagy, G.L. Jackson, T. Osborne, Supplemental ELM control in ITER through beryllium granule injection, Nucl. Mater. Energy 19 (2019) 34–41, https://doi.org/10.1016/j.nme.2019.02.005.

[9] R.P. Doerner, R.W. Conn, S.C. Luckhardt, F.C. Sze, J. Won, Outgassing from and deuterium retention in beryllium and Be/C mixed-material plasma-facing components, Fusion Eng. Des. 49-50 (2000) 183–188, https://doi.org/10.1016/S0920-3796(00)00421-X.

[10] R.P. Doerner, A.A. Grossman, S. Luckhardt, R. Seraydarian, F.C. Sze, D.G. Whyte, Mixed-material coating formation on plasma-facing components, J. Nucl. Mater. 266-269 (1999) 392–398, https://doi.org/10.1016/S0022-3115(98)00535-2.

[11] K. Ashida, K. Watanabe, Chemical compound formation and its analysis in the beryllium-carbon binary system at elevated temperatures, Fusion Eng. Des. 37 (2) (1997) 307–315, https://doi.org/10.1016/S0920-3796(97)00055-0.

[12] V. Amendola, M. Meneghetti, What controls the composition and the structure of nanomaterials generated by laser ablation in liquid solution? *Phys. Chem. Chem. Phys.* 15 (9) (2013) 3027–3046, https://doi.org/10.1039/c2cp42895d.

[13] A. Torrisi, M. Cutroneo, L. Torrisi, J. Vacík, Biocompatible nanoparticles production by pulsed laser ablation in liquids, J. Instrum. 15 (3) (2020), https://doi.org/10.1088/1748-0221/15/03/C03053.

[14] V. Altunal, Z. Yegingil, T. Tuken, T. Depci, A. Ozdemir, V. Guckan, N. Nur, K. Kurt, E. Bulur, Optically stimulated luminescence characteristics of BeO nanoparticles synthesized by sol-gel method, Radiat. Meas. 118 (2018) 54–66, https://doi.org/10.1016/j.radmeas.2018.08.009.

[15] X.-F. Wang, R.-C. Wang, C.-Q. Peng, T.-T. Li, B. Liu, Synthesis and sintering of beryllium oxide nanoparticles, Progr. Nat. Sci.: Mater. Int. 20 (2010) 81–86, https://doi.org/10.1016/S1002-0071(12)60011-2.

[16] S. Faraji, S. Feizi, A.A. Sabouri Dodaran, A. Alipour, P. Ashtari, M. Sharbatdaran, Beryllium oxide nanoparticles: synthesis, characterization, and thermoluminescence evaluation for gamma radiation detection, Radiochim. Acta 109 (11) (2021) 841–849, https://doi.org/10.1515/ract-2021-1081.

[17] S. Barcikowski, G. Compagnini, Advanced nanoparticle generation and excitation by lasers in liquids, PCCP 15 (9) (2013) 3022–3026, https://doi.org/10.1039/C2CP90132C.

[18] X. Song, K.L. Xiao, X.Q. Wu, G. Wilde, M.Q. Jiang, Nanoparticles produced by nanosecond pulse laser ablation of a metallic glass in water, J. Non-Cryst. Solids 517 (2019) 119–126, https://doi.org/10.1016/j.jnoncrysol.2019.05.009.

[19] V. Amendola, D. Amans, Y. Ishikawa, N. Koshizaki, S. Scirè, G. Compagnini, S. Reichenberger, S. Barcikowski, Room-temperature laser synthesis in liquid of oxide, metal-oxide core-shells, and doped oxide nanoparticles, Chem. – A Eur. J. 26 (42) (2020) 9206–9242, https://doi.org/10.1002/chem.202000686.

[20] M. Sakamoto, M. Fujistuka, T. Majima, Light as a construction tool of metal nanoparticles: synthesis and mechanism, *J. Photochem. Photobiol. C: Photochem. Rev.* 10 (1) (2009) 33–56, https://doi.org/10.1016/j.jphotochemrev.2008.11.002.

[21] E.V. Barmina, I.A. Sukhov, N.M. Lepekhin, Y.S. Priseko, V.G. Filippov, A. V. Simakin, G.A. Shafeev, Application of copper vapour lasers for controlling activity of uranium isotopes, Quantum Electron. 43 (6) (2013) 591–596, https://doi.org/10.1070/QE2013v043n06ABEH014879.

[22] I.A. Sukhov, G.A. Shafeev, E.V. Barmina, A.V. Simakin, V.V. Voronov, O.V. Uvarov, Hydrogen generation by laser irradiation of colloids of iron and beryllium in water, Quantum Electron. 47 (6) (2017) 533–538, https://doi.org/10.1070/QEL16325.

[23] F. Stokker-Cheregi, T. Acsente, I. Enculescu, C. Grisolia, Tungsten and aluminium nanoparticles synthesized by laser ablation in liquids, Digest J. Nanomater. Biostruct. 7 (4) (2012) 1569–1576.

[24] M. Reinelt, A. Allouche, M. Oberkofler, C.h. Linsmeier, Retention mechanisms and binding states of deuterium implanted into beryllium, New J. Phys. 11 (4) (2009) 043023, https://doi.org/10.1088/1367-2630/11/4/043023.

[25] D. Matveev, M. Wensing, L. Ferry, F. Virot, M. Barrachin, Y. Ferro, C. Linsmeier, Reaction-diffusion modeling of hydrogen transport and surface effects in application to single-crystalline Be, Nucl. Instrum. Methods Phys. Res., Sect. B 430 (2018) 23–30, https://doi.org/10.1016/j.nimb.2018.05.037.

[26] P. Wagener, J. Jakobi, C. Rehbock, V.S.K. Chakravadhanula, C. Thede, U. Wiedwald, M. Bartsch, L. Kienle, S. Barcikowski, Solvent-surface interactions control the phase structure in laser-generated iron-gold core-shell nanoparticles, Sci. Rep. 6 (1) (2016), https://doi.org/10.1038/srep23352.

[27] M.H. Mahdieh, B. Fattahi, Size properties of colloidal nanoparticles produced by nanosecond pulsed laser ablation and studying the effects of liquid medium and laser fluence, Appl. Surf. Sci. 329 (2015) 47–57, https://doi.org/10.1016/j.apsusc.2014.12.069.

[28] Rasband, W., and contributors, National Institute of Health, USA, Java 1.8.0_172 (64-bit). https://imagej.nih.gov/ij/.

[29] T. Tsuji, K. Iryo, N. Watanabe, M. Tsuji, Preparation of silver nanoparticles by laser ablation in solution: influence of laser wavelength on particle size, Appl. Surf. Sci. 202 (1-2) (2002) 80–85, https://doi.org/10.1016/S0169-4332(02)00936-4.

[30] J. Kim, D. Amaranatha Reddy, R. Ma, T.K. Kim, The influence of laser wavelength and fluence on palladium nanoparticles produced by pulsed laser ablation in deionized water, Solid State Sci. 37 (2014) 96–102, https://doi.org/10.1016/j.solidstatesciences.2014.09.005.

[31] P. Chewchinda, T. Tsuge, H. Funakubo, O. Odawara, H. Wada, Laser wavelength effect on size and morphology of silicon nanoparticles prepared by laser ablation in liquid, Jpn. J. Appl. Phys. 52 (2013), 025001, https://doi.org/10.7567/JJAP.53.039201.

[32] M. Dell'Aglio, R. Gaudiuso, O. De Pascale, A. De Giacomo, Mechanisms and processes of pulsed laser ablation in liquids during nanoparticle production, Appl. Surf. Sci. 348 (2015) 4–9, https://doi.org/10.1016/j.apsusc.2015.01.082.

[33] F. Taccogna, Nucleation and growth of nanoparticles in a plasma by laser ablation in liquid, J. Plasma Phys. 81 (5) (2015), https://doi.org/10.1017/S0022377815000793.

[34] M. Dell'Aglio, A. De Giacomo, Plasma charging effect on the nanoparticles releasing from the cavitation bubble to the solution during nanosecond Pulsed Laser Ablation in Liquid, Appl. Surf. Sci. 515 (2020) 146031, https://doi.org/10.1016/j.apsusc.2020.146031.

[35] S. Reich, P. Schönfeld, P. Wagener, A. Letzel, S. Ibrahimkutty, B. Gökce, S. Barcikowski, A. Menzel, T. dos Santos Rolo, A. Plech, Pulsed laser ablation in liquids: Impact of the bubble dynamics on particle formation, J. Colloid Interface Sci. 489 (2017) 106–113, https://doi.org/10.1016/j.jcis.2016.08.030.

[36] C.-Y. Shih, R. Streubel, J. Heberle, A. Letzel, M.V. Shugaev, C. Wu, M. Schmidt, B. Gökce, S. Barcikowski, L.V. Zhigilei, Two mechanisms of nanoparticle generation in picosecond laser ablation in liquids: the origin of the bimodal size distribution, Nanoscale 10 (15) (2018) 6900–6910, https://doi.org/10.1039/C7NR08614H.

[37] K. Sugiyama, K. Krieger, C.P. Lungu, J. Roth, Hydrogen retention in ITER relevant mixed material layers, J. Nucl. Mater. 390-391 (2009) 659–662, https://doi.org/10.1016/j.jnucmat.2009.01.183.

[38] A.A. Haasz, J.W. Davis, Deuterium retention in beryllium, molybdenum and tungsten at high fluences, J. Nucl. Mater. 241–243 (1997) 1076–1081, https://doi.org/10.1016/S0022-3115(97)80197-3.

[39] A. Manhard, K. Schmid, M. Balden, W. Jacob, Influence of the microstructure on the deuterium retention in tungsten, J. Nucl. Mater. 415 (1) (2011) S632–S635.

[40] G. De Temmerman, M.J. Baldwin, R.P. Doerner, D. Nishijima, K. Schmid, An empirical scaling for deuterium retention in co-deposited beryllium layers, Nucl. Fusion 48 (7) (2008) 075008, https://doi.org/10.1088/0029-5515/48/7/075008.

[41] A. Založnik, M.J. Baldwin, R.P. Doerner, T. Schwarz-Selinger, S. Brezinsek, The influence of helium on deuterium retention in beryllium co-deposits, J. Nucl. Mater. 512 (2018) 25–30, https://doi.org/10.1016/j.jnucmat.2018.09.032.

[42] R.A. Anderl, R.A. Causey, J.W. Davis, R.P. Doerner, G. Federici, A.A. Haasz, G. R. Longhurst, W.R. Wampler, K.L. Wilson, Hydrogen isotope retention in beryllium for tokamak plasma-facing applications, J. Nucl. Mater. 273 (1) (1999) 1–26, https://doi.org/10.1016/S0022-3115(99)00022-7.

[43] G. De Temmerman, K. Heinola, D. Borodin, S. Brezinsek, R.P. Doerner, M. Rubel, E. Fortuna-Zaleśna, C. Linsmeier, D. Nishijima, K. Nordlund, M. Probst, J. Romazanov, E. Safi, T. Schwarz-Selinger, A. Widdowson, B.J. Braams, H.-K. Chung, C. Hill, Data on erosion and hydrogen fuel retention in Beryllium plasma-facing materials, Nucl. Mater. Energy 27 (2021) 100994, https://doi.org/10.1016/j.nme.2021.100994.

[44] A. Založnik, M.J. Baldwin, R.P. Doerner, G. De Temmerman, R.A. Pitts, Improved scaling law for the prediction of deuterium retention in beryllium co-deposits, Nucl. Fusion 62 (3) (2022) 036006, https://doi.org/10.1088/1741-4326/ac4775.